A 1 year record of carbonaceous aerosols from an urban site in the Indo-Gangetic Plain: Characterization, sources, and temporal variability

Kirpa Ram,[1] M. M. Sarin,[1] and S. N. Tripathi[2]

Received 12 March 2010; revised 8 July 2010; accepted 14 July 2010; published 30 December 2010.

[1] This study presents a comprehensive 1 year (January 2007–March 2008) data set on the chemical composition of ambient aerosols collected from an urban location (Kanpur) in the Indo-Gangetic Plain (IGP) and suggests that the varying strength of the regional emission sources, boundary layer dynamics, and formation of secondary aerosols all contribute significantly to the temporal variability in the mass concentrations of elemental carbon (EC), organic carbon (OC), and water-soluble OC (WSOC). On average, carbonaceous aerosols contribute nearly one third of the PM_{10} mass during winter, whereas their fractional mass is only ~10% during summer. A three- to four-fold increase in the OC and K^+ concentrations during winter and a significant linear relation between them suggest biomass burning (wood fuel and agricultural waste) emission as a dominant source. The relatively high OC/EC ratio (average: 7.4 ± 3.5 for n = 66) also supports that emissions from biomass burning are overwhelming for the particulate OC in the IGP. The WSOC/OC ratios vary from 0.21 to 0.70 over the annual seasonal cycle with relatively high ratios in the summer, suggesting the significance of secondary organic aerosols. The long-range transport of mineral aerosols from Iran, Afghanistan, and the Thar Desert (western India) is pronounced during summer months. The temporal variability in the concentrations of selected inorganic constituents and neutralization of acidic species (SO_4^{2-} and NO_3^-) by NH_4^+ (dominant during winter) and Ca^{2+} (in summer) reflect conspicuous changes in the source strength of anthropogenic emissions.

Citation: Ram, K., M. M. Sarin, and S. N. Tripathi (2010), A 1 year record of carbonaceous aerosols from an urban site in the Indo-Gangetic Plain: Characterization, sources, and temporal variability, *J. Geophys. Res.*, *115*, D24313, doi:10.1029/2010JD014188.

1. Introduction

[2] Carbonaceous aerosols, consisting of organic carbon (OC) and elemental carbon (EC), are the major components of atmospheric particulate matter (PM) and constitute ~30–70% of the fine (<1 μm) mass in urban atmospheres [*Cao et al.*, 2003; *Fuzzi et al.*, 2006; *Rengarajan et al.*, 2007]. The real-time and long-term measurements of carbonaceous aerosols from South Asia are rather sparse (limited to only a few months of data) and inadequately represented in the literature [*Chowdhury et al.*, 2007; *Miyazaki et al.*, 2009; *Ram and Sarin*, 2010; *Rengarajan et al.*, 2007; *Sheesley et al.*, 2003]. Recently, *Ganguly et al.* [2009] had argued in favor of ground-based long-term measurements of carbonaceous aerosols to improve the parameterization and validation of optical properties retrieved from satellites. Furthermore, the relative amount of OC and EC in the atmosphere and OC/EC ratios are the important parameters for the assessment of direct/indirect impacts of aerosols on the regional scale radiative forcing [*Novakov et al.*, 2005]. The OC/EC ratios currently used in the radiative transfer models are largely derived based on the emission inventories of organic aerosols. However, these ratios depend on the fuel type, quantity, and, more importantly, their combustion efficiency [*Bond et al.*, 2007; *Streets et al.*, 2004]. These parameters are highly variable depending on the geographical location; thus, there is a need for systematic and long-term measurements of carbonaceous aerosols from the South Asian region.

[3] The Indo-Gangetic Plain (IGP), extending from 21.75°N, 74.25°E to 31.0°N, 91.5°E, is one of the most populated and polluted regions in northern India. The large-scale urbanization, land use changes, industrial activities, and regional emission sources (biomass burning and fossil fuel) contribute to the high aerosol loading over the entire IGP. The Gangetic Plain experiences extreme variability in the climate over the annual seasonal cycle. The dense fog and haze weather conditions during winter, intense convective mixing in the summer, and transport of mineral dust from Pakistan, Afghanistan, and the Thar Desert (in western India) impart a characteristic seasonal variability to the

[1]Physical Research Laboratory, Ahmedabad, India.
[2]Department of Civil Engineering, Indian Institute of Technology, Kanpur, India.

0148-0227/10/2010JD014188

aerosol composition. In this context, our study is relevant and presents a comprehensive 1 year data set on the mass concentrations of OC, EC, water-soluble OC (WSOC), and inorganic species (K^+, NH_4^+, Ca^{2+}, NO_3^-, and SO_4^{2-}) in the ambient aerosols from an urban location (Kanpur) in the Indo-Gangetic Plain. It is implicit that satellite and optical observations do not provide information with regard to OC/EC and WSOC/OC ratios and the formation of secondary organic aerosols (SOA).

2. Experiment

2.1. Site Description

[4] The sampling site at Kanpur (26.5°N, 80.3°E, 142 m above mean sea level), representing an urban environment, is located in the central part of the Indo-Gangetic Plain. The aerosol sampling, carried out over a period of 14 months (January 2007–March 2008), was set up on the third floor of the Environmental Engineering Laboratory (~15 m above ground level) located inside the Indian Institute of Technology campus and upwind of the emission sources from the city. The widespread impact of biomass burning emissions on the regional air quality is significantly pronounced in winter due to the crop harvesting season and a common practice of wood fuel burning for domestic use. A shallow boundary layer height during the winter, typically 500–800 m [*Nair et al.*, 2007], and the Himalayan mountain range parallel to the Gangetic Plain confine anthropogenic aerosols within the lower atmosphere. The surface level low pressure in northwestern India, aided by the westerly and northwesterly winds and high ambient temperatures, is mainly responsible for the long-range transport of mineral aerosols during the summer months [*Mishra and Tripathi*, 2008; *Singh et al.*, 2005].

2.2. Analytical Measurements

[5] The ambient aerosols (PM_{10}, particulate matter with aerodynamic diameter <10 μm) were collected on precombusted (at 550°C for ~6 h) tissuquartz filters (PALLFLEX™, 2500 QAT-UP; size: 20.0 × 25.4 cm^2) using a high-volume sampler operated at a flow rate of 1.0 ± 0.1 m^3 min^{-1}. The PM_{10} sampler was periodically calibrated (once every 2–3 weeks) to check on variations, if any, in the flow rate. All samples (n = 66) were collected during daytime and integrated for ~8–10 h; the volume of air ranged from ~500–600 m^3. The sampling frequency of one sample every fifth day was maintained during January–February and October–December 2007, and increased to two samples per week during March–June 2007, when mineral dust is relatively abundant. Simultaneously, meteorological parameters were recorded by an automatic weather station (Envirotech Pvt. Ltd., New Delhi, India); wherein temperature, wind speed, and relative humidity (RH) were measured with an accuracy of 0.1°C, 0.1 ms^{-1}, and 3%, respectively. The aerosol sampling was suspended during the wet-season (July–September) when the southwest monsoonal rains cause efficient washout of the atmosphere.

2.2.1. PM_{10} Mass Concentration

[6] All filters were equilibrated in a laminar flow bench for ~15–20 h under constant relative humidity (35 ± 5%) and temperature (22 ± 1°C) conditions prior to their weighing on a balance. The total PM mass (μg m^{-3}) was obtained from subtracting the blank filter weight from the total weight and divided by the total volume of air (m^{-3}).

2.2.2. OC and EC

[7] The mass concentrations of OC and EC in ambient aerosols are assessed by an EC-OC analyzer (Sunset Laboratory, USA) using the thermo-optical transmittance protocol. The analytical details of the measurements have been described in our earlier publications [*Ram et al.*, 2008; *Rengarajan et al.*, 2007]. Briefly, a filter aliquot (1.5 cm^2) is stepwise heated in an inert (100% He) atmosphere followed by heating in an oxidizing medium (10% O_2 + 90% He, vol/vol). The carbon fraction evolved during the heating cycle is oxidized to CO_2, converted to methane (CH_4), and measured using a flame-ionization detector. The transmittance of a laser source (678 nm) through the sample filter is continuously monitored and return of the transmittance to its initial value on the thermograph is taken as a split line between OC and EC. The carbon fraction evolved prior to the split line is defined as OC and the latter component is referred as EC; both OC and EC components are subsequently corrected for the pyrolysed carbon. Along with the samples, blank filters are also run in a similar manner to establish the detection limit of OC and to make suitable correction for the contribution of OC from the tissue quartz filters. The average concentration of OC from the blank filters was 1.2 ± 0.4 μgC cm^{-2} for n = 13, with no measurable signal for EC. The detection limit for OC was calculated as three times the standard deviation of the blank concentration, whereas the detection limit for EC was assumed to be equal to the minimum signal (0.2 μgC cm^{-2}) measurable on the instrument. The detection limits for OC and EC thus correspond to 0.8 and 0.15 μgC m^{-3}, respectively, for an average air volume of ~600 m^3.

2.2.3. WSOC

[8] For WSOC, one-fourth of the filter (~105 cm^2 area) is soaked in 50 mL Milli-Q water (resistivity: 18.2 MΩ cm) for nearly 6–8 h, with an intermittent ultrasonic treatment to disintegrate the aerosol particles from the filters. The resulting water extract is filtered through PALLFLEX™ glass fiber filter (Diameter: 47 mm), transferred to a precleaned glass vial, and analyzed for WSOC on TOC analyzer (Shimadzu, Model TOC-5000A). The analytical procedure includes injecting 25 μL of water extract into the furnace, maintained at a temperature of 680°C, and oxidation to CO_2 using platinum catalyst. The evolved CO_2 is measured using a nondispersive infrared (NDIR) detector to assess the total carbon (TC) content. Another aliquot of the solution (100 μL) is acidified with 25% phosphoric acid (25% H_3PO_4, vol/vol) and the evolved CO_2 is referred as inorganic carbon (IC). The difference between the two sets of measurements (i.e., TC and IC) is used as a measure of WSOC in the aerosol samples. The response of the NDIR detector for TC and IC measurements is calibrated using the standard solutions of potassium hydrogen phthalate and sodium carbonate-bicarbonate mixture (Na_2CO_3+$NaHCO_3$; 1:1 vol/vol), respectively. Each analysis of TC and IC was repeated three times to achieve a coefficient of variation (CV) less than 2%. The replicate analyses of the water extracts provide relative standard deviation (RSD) of 3% and 5% for TC and IC, respectively (for n = 14). The extraction of blank filters was simultaneously processed and the average values were ascertained to be 1.1 ± 0.8 ppm and 350 ± 40 ppb (±1σ for n = 7) for TC and IC, respectively.

2.2.4. Water-Soluble Ionic Species (WSIS)

[9] The water-soluble cations (Na^+, K^+, NH_4^+, Ca^{2+}, and Mg^{2+}) and anions (Cl^-, SO_4^{2-}, and NO_3^-) in the aerosol samples were analyzed using an ion-chromatography technique. An aliquot of the water extract (extracted similar to that used for the analysis of WSOC) is transferred to a precleaned polyethylene bottle and stored until the analysis. The anions are separated using 1.8 mM Na_2CO_3/1.7 mM $NaHCO_3$ as an eluent on AS-14 chromatography column in conjunction with the anion self-regenerating suppressor. For cations, 20 mM methanesulfonic acid is used as an eluent on CS-12 column, connected in series with the cation self-regenerating suppressor. The relevant analytical details for the analyses of water-soluble ionic constituents have been described in our earlier publications [*Rastogi and Sarin*, 2006; *Rengarajan et al.*, 2007]. The blank filters are also analyzed to assess the net concentrations of ionic species in the samples. The replicate analysis (n = 11) was better than 3% for K^+, Ca^{2+}, Mg^{2+}, Cl^-, SO_4^{2-}, and NO_3^- and 6% for NH_4^+.

[10] An aliquot of the water extract of aerosol samples was used to measure bicarbonate ion (HCO_3^-) in an auto-titration system (Metrohm, model 702 SM Titrino) by using a fixed endpoint acid titration (at pH = 4.3) with 0.005 M HCl. The system calibration, in the range of 0 to 1000 μM, was performed with freshly prepared solution of sodium carbonate (Na_2CO_3). The detection limit for bicarbonate, based on the variability in the blank filters, was 45 μM. The CV for several repeat measurements (n = 9) was estimated to be better than 2%.

3. Results and Discussion

3.1. Meteorology and Back Trajectory Analysis

[11] The regional meteorology, topography, and emission sources (natural and anthropogenic) play an important role in determining the spatiotemporal variability in the aerosol mass concentration and chemical composition. The flat topography of the Indo-Gangetic Plain (extending from northeast to northwest and parallel to the Himalayan range), the moderate winds, and a shallow boundary layer height during winter favor an efficient trapping of the aerosols in the lower atmosphere. The seasonal rainfall during the period of southwest monsoon (late June–September) accounts for ~70% of the annual precipitation, with very little rainfall occurring during the winter (December–February). On the basis of the regional meteorology, the temporal variability in the aerosol composition has been discussed in terms of four different seasonal patterns referred to as winter (December–February), summer/premonsoon (April–June), monsoon (late June–September) and postmonsoon (October–November). It is relevant to state that the annual seasonal cycle, as defined in this study, represents the tropical climate of the Gangetic Plain. March represents transition phase between winter and summer. In general, the major wind regime during the sampling period was northwesterly, and occasionally from the northeast and southwest (Figure 1 and Table 1). The average RH was about 70% and the winds were generally weak during the winter and postmonsoon compared to those during the summer season (Table 1).

[12] The 5 day back trajectory analysis was performed (at three different heights 500, 1000, and 1500 m above ground level) to track the origin and transport of air masses arriving at the sampling site. The air mass trajectories were obtained from the final run data archive of Global Data Assimilation System model using NOAA Air Resource Laboratory (ARL) Hybrid Single-Particle Lagrangian Integrated Trajectory (HYSPLIT) Model (available at http://www.arl.noaa.gov/ready/hysplit4.html (accessed via NOAA ARL Real-time Environmental Applications and Display sYstem (READY) website http://ready.arl.noaa.gov)). The back trajectories computed for the specific sampling dates (28 March, 2 June, 16 and 20 Nov, and 1 and 16 Dec, Figure 2) indicate localized as well as long-range transport of aerosols. The long-range transport of mineral dust originating from Iran, Afghanistan, Pakistan, and the Thar Desert (western India) is a characteristic feature during the summer months, whereas localized air masses during winter and post-monsoon indicate the dominance of anthropogenic emission sources. The back trajectories, presented in Figure 2, are considered representative of the seasonal feature and exhibit characteristic differences with respect to aerosol composition (Table 2).

3.2. Source Characterization and Aerosol Composition

[13] It is well recognized that K^+ is an ideal tracer for the source characterization of carbonaceous aerosols from biomass burning emissions [*Andreae*, 1983; *Andreae and Merlet*, 2001]. However, appropriate corrections for aerosol K^+ derived from sea salt and mineral dust are essential [*Chester*, 1990]. In the absence of a biomass burning source, one would expect the contribution from mineral dust to be more in the summer (April–June) due to the long-range transport from arid regions. The seasonal average mass concentrations of carbonaceous and water-soluble inorganic species are summarized in Table 3. During summer months, K^+ content in the majority of the samples is relatively low (0.33 to 0.93 μg m^{-3}; Table 3) compared to that during the winter and postmonsoon (~2.0 μg m^{-3}). The mineral dust content in the aerosols (inferred based on the measured concentration of Ca^{2+}) during summer and winter seasons is significantly different; the relatively low contribution of dust during postmonsoon and winter would result in lower concentration of aerosol K^+. On the basis of the average Na^+ concentration of 0.42 ± 0.32 μg m^{-3} (Table 3) and assuming K^+/Na^+ molar ratio of 0.037 in seawater [*Chester*, 1990], the contribution of K^+ derived from sea salt is insignificant (~0.01 μg m^{-3}). Thus, K^+ from sea salt contributes no more than 3% and 1% of the total K^+ during summer and winter seasons, respectively. The mass concentration of OC exhibits a linear relation with K^+ in the samples collected during winter and postmonsoon (R^2 = 0.79 and 0.50, respectively; Figure 3a); suggesting that K^+ and OC are derived from a common source (biomass burning). However, K^+ and EC concentrations show a large scatter, indicating multiple sources of EC (Figure 3b). Furthermore, the relationship between K^+ and OC (Figure 3c) as well as K^+ and EC (Figure 3d) are poor for the samples collected during summer (April–June).

[14] Dust storms are very common over the IGP during summer (April–June). The PM_{10} mass concentration can increase to as high as 1000 μg m^{-3} during dust storm events at Kanpur [*Chinnam et al.*, 2006]. For a semi-arid urban location in western India, *Rastogi and Sarin* [2006] reported

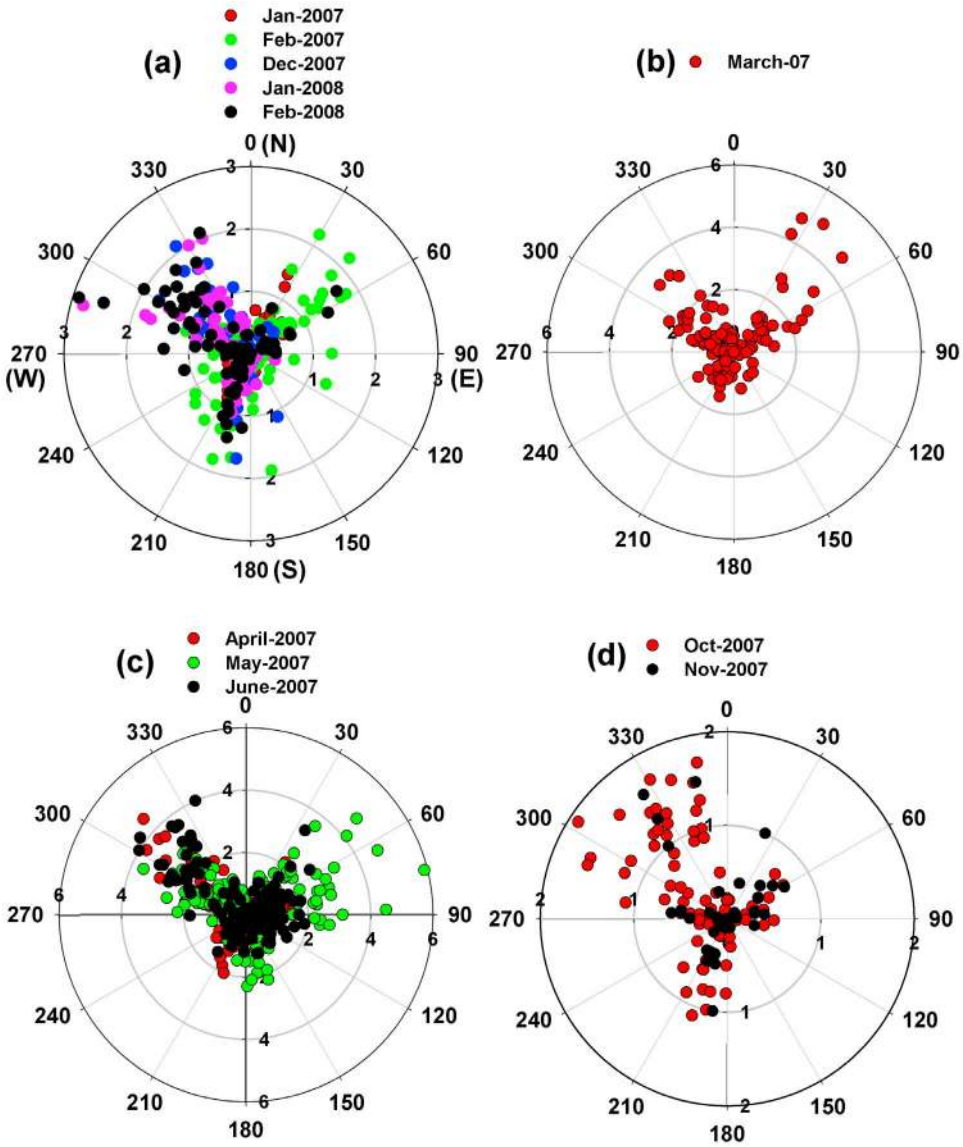

Figure 1. Seasonal wind-rose plot for the sampling period from January 2007 to February 2008: (a) winter (December–February), (b) spring (March), (c) summer (April–June) and (d) postmonsoon (October–November). N, north; E, east; S, south; W, west.

that mineral dust contributes ~70–80% of the total suspended particulate matter throughout the year. A significant fraction of calcium (Ca) is soluble in water and the measured Ca^{2+} is generally used as an indicator of mineral aerosols [*Lin et al.*, 2007; *Rastogi and Sarin*, 2006]. The measured Ca^{2+} concentration shows a significant linear trend with PM_{10} mass for the samples collected during March and the summer season (R^2 = 0.67; Figure 3e). However, a large scatter is

Table 1. Meteorological Data During the Sampling Period at Kanpur and the Source Defining Criterion Based on Measured Chemical Species[a]

Months	T (°C)	WS (ms^{-1})	WD	RH (%)	Source Defining Criterion	Potential Sources of Aerosols
Dec–Feb	15.7 ± 5.6 (5.2–29.6)	0.5 ± 0.5 (0.0–2.9)	192 ± 97 (6–355)	70 ± 24 (17–100)	High K^+, low Ca^{2+} concentrations, and higher OC/EC ratios	Biomass burning emission
Mar	22.9 ± 5.2 (15.4–30.6)	0.8 ± 0.5 (0.1–5.1)	196 ± 37 (134–286)	56 ± 19 (28–84)	Relatively low K^+ and OC/EC ratios, high Ca^{2+} concentrations	Vehicular emission + mineral dust
Apr–Jun	31.5 ± 5.4 (17.3–44.1)	1.0 ± 1.0 (0.1–6.1)	177 ± 99 (15–355)	43 ± 13 (26–60)	Relatively high Ca^{2+} concentrations, higher OC/EC ratios and low K^+	Mineral dust
Oct–Nov	22.9 ± 6.3 (9.3–35.5)	0.3 ± 0.5 (0.0–3.5)	170 ± 100 (1–359)	67 ± 24 (17–100)	High K^+, low Ca^{2+} concentrations, and higher OC/EC ratios	Biomass burning emission

[a]Numbers within bracket present the range of values.
[b]T, temperature; WS, wind speed; WD, wind direction; RH, relative humidity.

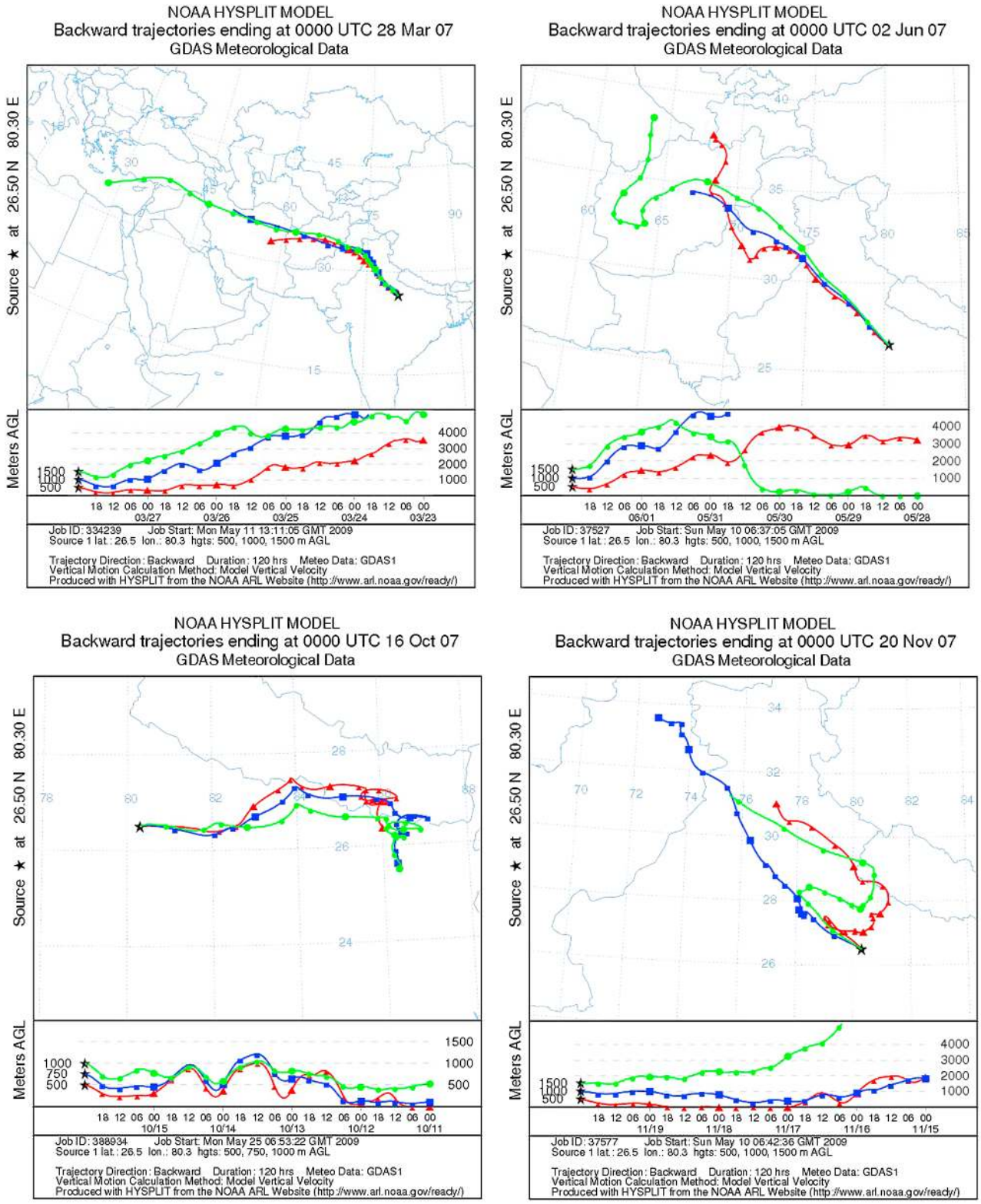

Figure 2. Five day back trajectory analyses (using NOAA HYbrid Single-Particle Lagrangian Integrated Trajectory (HYSPLIT) Model accessed via NOAA ARL Real-time Environmental Applications and Display sYstem (READY) website (http://ready.arl.noaa.gov) at http://www.arl.noaa.gov/ready/hysplit4.html) for the selected sampling dates (see also Table 2) in order to ascertain the long-range transport of air masses.

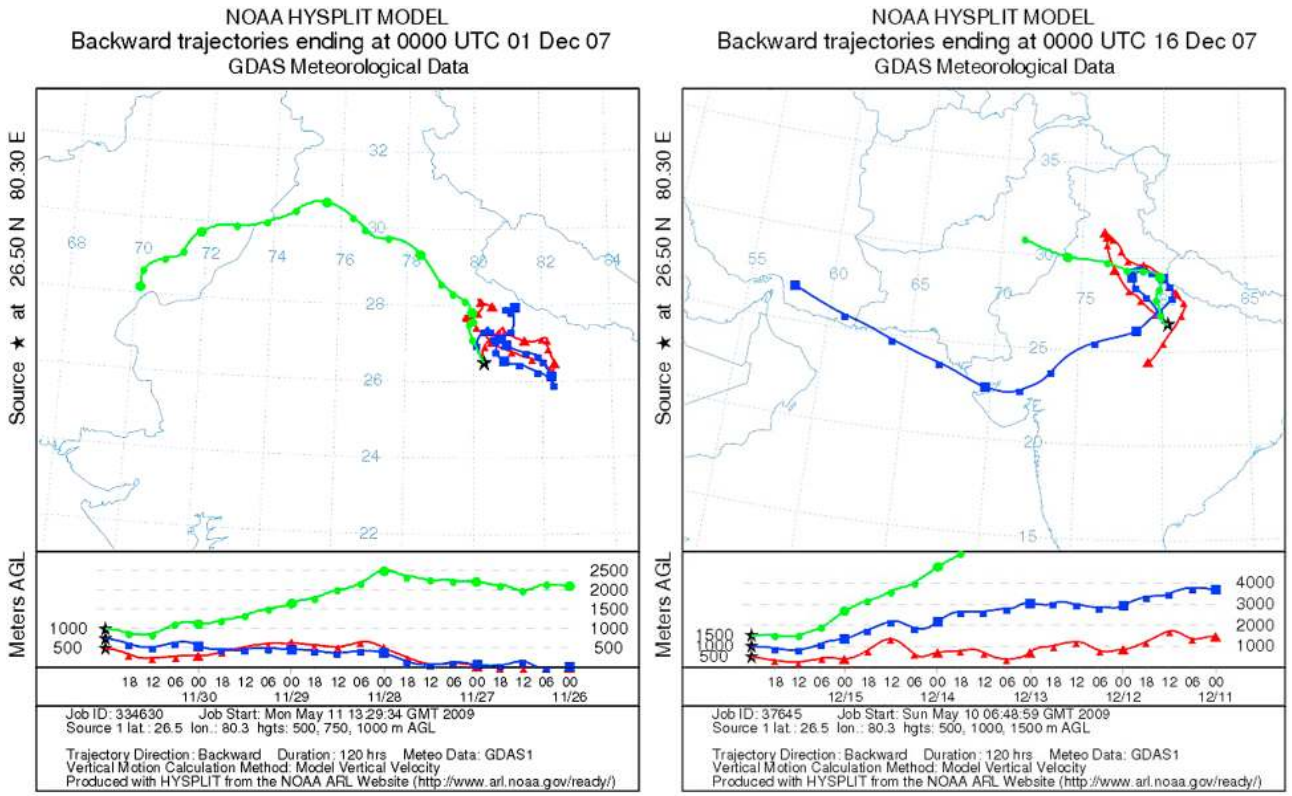

Figure 2. (continued)

observed for the samples collected during winter and postmonsoon (Figure 3f). Furthermore, the concentration of Ca^{2+} is significantly higher in March and the summer months than in the postmonsoon and winter (Table 3). This is further evident from the low total carbonaceous aerosols (TCA)-to-Ca^{2+} mass ratio in the summer (TCA/Ca^{2+} = 15 ± 8) compared to significantly high ratio during the winter (62 ± 37). The assessment of TCA is further discussed in section 3.3. The potential sources of aerosols and their defining criteria for the sampling site (Kanpur) are summarized in Table 1.

[15] On the basis of the measured concentrations of chemical species (K^+ and Ca^{2+}) and OC/EC and TCA/Ca^{2+} ratios in aerosols, combined with the back trajectory analyses (Figure 2), it can be inferred that the aerosol composition during the winter (December–February) and postmonsoon (October–November) is dominated by the biomass burning emissions, while aerosol composition during summer (April–June) is dominated by the mineral dust. The chemical composition of aerosols for the 6 days (as selected in Figure 2) is presented in Table 2. In general, relatively low contribution from TCA and WSIS (derived from sum of the cations and anions) is evident during summer compared to that in the postmonsoon and winter.

3.3. Seasonal Variability in PM_{10} Mass

[16] The monthly average PM_{10} mass, along with OC, EC, and WSOC concentrations and their ratios, are given in Table 4. The PM_{10} (range: 42–312 $\mu g\ m^{-3}$), TCA, and WSIS mass exhibit a large temporal variability (Figures 4a, 4b, and 4c, respectively). In general, higher PM_{10} mass is associated with the samples collected during the postmonsoon (October–November) and winter (December–February), whereas relatively low concentrations are characteristic of the samples collected during March and the summer months (April–June). The seasonal variability in PM_{10} mass can be explained as a combined effect of local emission sources and the prevailing meteorological conditions (wind regimes and boundary layer dynamics). The carbonaceous and ionic species contribute significantly to the PM_{10} mass concentration during winter and postmonsoon. The mass of TCA is estimated by adding the concentrations of organic matter (OM) and EC, whereas organic matter content is assessed based on organic carbon measured in the aerosols (i.e.,

Table 2. Representative Concentrations of Measured Chemical Species for Selected Days (For Which Back Trajectory Analyses Were Performed)

Sampling Dates	PM_{10} ($\mu g\ m^{-3}$)	OC/EC	TCA/Ca^{2+}	% TCA of PM_{10}	% WSIS of PM_{10}
28 Mar 07	274.8	2.8	22.3	26	8
2 Jun 07	221.8	6.6	7.3	10	7
16 Oct 07	104.5	6.2	22.8	36	20
20 Nov 07	308.2	8.8	60.7	24	9
1 Dec 07	252.0	11.6	492.0	38	31
16 Dec 07	312.5	10.0	22.5	26	19

Table 3. Seasonal Average Mass Concentrations of Carbonaceous Species and Water-Soluble Inorganic Species ($\pm 1\sigma$) at Kanpur[a]

Months[b]	n[c]	OC	EC	WSOC	Na^+	NH_4^+	K^+	Ca^{2+}	Mg^{2+}	Cl^-	NO_3^-	SO_4^{2-}	HCO_3^-	NH_4^+/SO_4^{2-}	NF (NH_4^+)	NF (Ca^{2+})	NF (Mg^{2+})
Dec–Feb	22	40.4 ± 16.6 (34.0)	4.9 ± 1.5 (4.4)	15.3 ± 7.6 (13.4)	0.5 ± 0.4 (0.4)	8.9 ± 4.5 (7.2)	1.9 ± 0.9 (1.5)	1.4 ± 1.1 (1.0)	0.2 ± 0.2 (0.2)	3.1 ± 2.3 (2.1)	17.1 ± 1.9 (12.5)	12.7 ± 5.1 (11.7)	2.1 ± 1.8 (1.3)	3.6 ± 1.5 (3.5)	0.87 ± 0.22 (90)	0.12 ± 0.10 (0.08)	0.03 ± 0.02 (0.02)
March	9	19.9 ± 10.3 (17.6)	5.8 ± 4.1 (4.6)	6.4 ± 2.5 (6.0)	0.4 ± 0.4 (0.3)	1.5 ± 1.3 (1.2)	0.5 ± 0.6 (0.4)	2.2 ± 1.5 (1.6)	0.3 ± 0.2 (0.2)	0.5 ± 0.4 (0.3)	2.8 ± 2.9 (1.6)	8.6 ± 4.6 (7.8)	3.3 ± 3.1 (2.0)	0.8 ± 0.3 (0.7)	0.36 ± 0.14 (0.29)	0.40 ± 0.14 (0.39)	0.09 ± 0.02 (0.08)
Apr–Jun	25	13.4 ± 4.3 (12.8)	2.1 ± 0.9 (1.9)	6.6 ± 2.0 (6.2)	0.4 ± 0.1 (0.3)	1.5 ± 0.9 (1.2)	0.6 ± 0.3 (0.6)	2.0 ± 1.1 (1.7)	0.2 ± 0.1 (0.2)	0.3 ± 0.2 (0.3)	2.2 ± 0.7 (2.1)	6.0 ± 1.9 (5.7)	4.7 ± 5.1 (4.2)	1.3 ± 0.6 (1.4)	0.49 ± 0.22 (0.53)	0.53 ± 0.30 (0.41)	0.10 ± 0.03 (0.09)
Oct–Nov	10	29.8 ± 9.5 (28.6)	4.1 ± 1.3 (3.9)	15.6 ± 4.6 (15.1)	0.3 ± 0.1 (0.3)	6.3 ± 1.9 (6.0)	2.0 ± 1.4 (1.8)	1.4 ± 0.4 (1.4)	0.2 ± 0.1 (0.2)	0.5 ± 0.3 (0.4)	6.0 ± 3.9 (5.0)	14.4 ± 4.4 (13.8)	1.4 ± 1.1 (1.2)	2.4 ± 0.4 (2.2)	0.88 ± 0.05 (0.89)	0.16 ± 0.06 (0.14)	0.04 ± 0.02 (0.03)

[a]The NH_4^+/SO_4^{2-} molar ratio and neutralization factors (NF) for NH_4^+, Ca^{2+} and Mg^{2+} are also given. Numbers within parentheses are median values. OC, EC, WSOC, Na^+, NH_4^+, K^+, Ca^{2+}, Mg^{2+}, Cl^-, NO_3^-, SO_4^{2-}, and HCO_3^- are given in $\mu g\ m^{-3}$.
[b]No samples were collected during July–September; time period characterized by SW monsoon.
[c]Number of samples collected during each season.

OM = 1.6 × OC). Although a wide range of values for OM/OC ratios (1.2 to 2.1) have been reported in the literature [*Turpin and Lim*, 2001], a ratio of 1.6 has been suggested for urban aerosols [*Cao et al.*, 2003; *Rengarajan et al.*, 2007].

[17] The contribution of TCA to PM_{10} mass is as high as 60% in some of the samples collected during winter (e.g., on 12 February 2008, day of year: 43; Figure 4d). Although the mass concentration of PM_{10} is relatively low during the summer compared to that in the winter, an increasing trend from February to June (Figure 5a) is attributed to the dominant contribution of mineral aerosols. The temporal variability in the mass concentration of TCA ($\mu gC\ m^{-3}$) and its contribution to PM_{10} are shown in Figure 5. As evident from Figure 5b, TCA contribution decreases by a factor of two during the summer compared to that in the winter. The WSIS mass contributes ~20% of PM_{10} during winter, whereas its contribution is only 10% during summer (Figure 4d).

[18] On the basis of the satellite retrieval and ground-based measurements of optical properties, relatively high values of aerosol optical depth (AOD) have been reported over the IGP [*Chinnam et al.*, 2006; *Dey and Tripathi*, 2008; *Jethva et al.*, 2005]. AOD values ranging from 0.6 to 1.2 (at 550 nm) during summer with relatively low fine-mode aerosol fraction, suggesting the dominance of coarse-mode, have been reported by *Jethva et al.* [2005]. However, the fine-mode aerosols (derived from anthropogenic emissions) dominate PM_{10} mass and result in higher AOD values during winter at Kanpur [*Jethva et al.*, 2005]. *Tare et al.* [2006] suggested that as much as 83% of the PM_{10} mass concentration at Kanpur is derived from the fine-mode particles (<1 μm) during the field campaign conducted in December 2004. However, there are no measurements of carbonaceous species reported in these studies except those of black carbon (BC) using an Aethalometer. It is important to note that organic carbon is a major constituent of the carbonaceous aerosols at urban locations in the Indo-Gangetic Plain and contributes significantly to the PM_{10} mass during winter [*Rengarajan et al.*, 2007]. In this study, TCA and WSIS together account for ~70% of the PM_{10} mass (Figure 4d), suggesting the dominance of carbonaceous aerosols during winter and postmonsoon.

3.4. Mass Concentrations of EC, OC, and OC/EC Ratio

[19] The EC and OC concentrations exhibit a large temporal variability during the sampling period (January 2007–March 2008), and their mass concentrations varied from 0.7 to 14.4 $\mu gC\ m^{-3}$ (Figure 6a) and 8.3 to 81.2 $\mu gC\ m^{-3}$ (Figure 6b), respectively. The annual average EC and OC concentrations, 3.8 ± 2.3 and 25.8 ± 16.1 $\mu gC\ m^{-3}$, respectively, account for 2.5% and ~16% of the PM_{10} mass at the study site (Kanpur) in the IGP. The seasonal average mass concentrations of EC and OC are presented in Table 3. The highest EC concentration (14.4 $\mu gC\ m^{-3}$, Figure 6a) was recorded in March 2007, whereas the highest OC concentration (81.2 $\mu gC\ m^{-3}$, Figure 6b) was observed in the sample collected during December 2007.

[20] On a seasonal basis, TCA accounts for ~38%, 17%, and 31% of the PM_{10} mass during winter, summer, and postmonsoon, respectively. The average EC and OC concentrations during postmonsoon and winter are two to three times higher than those in the summer (Table 3) due to

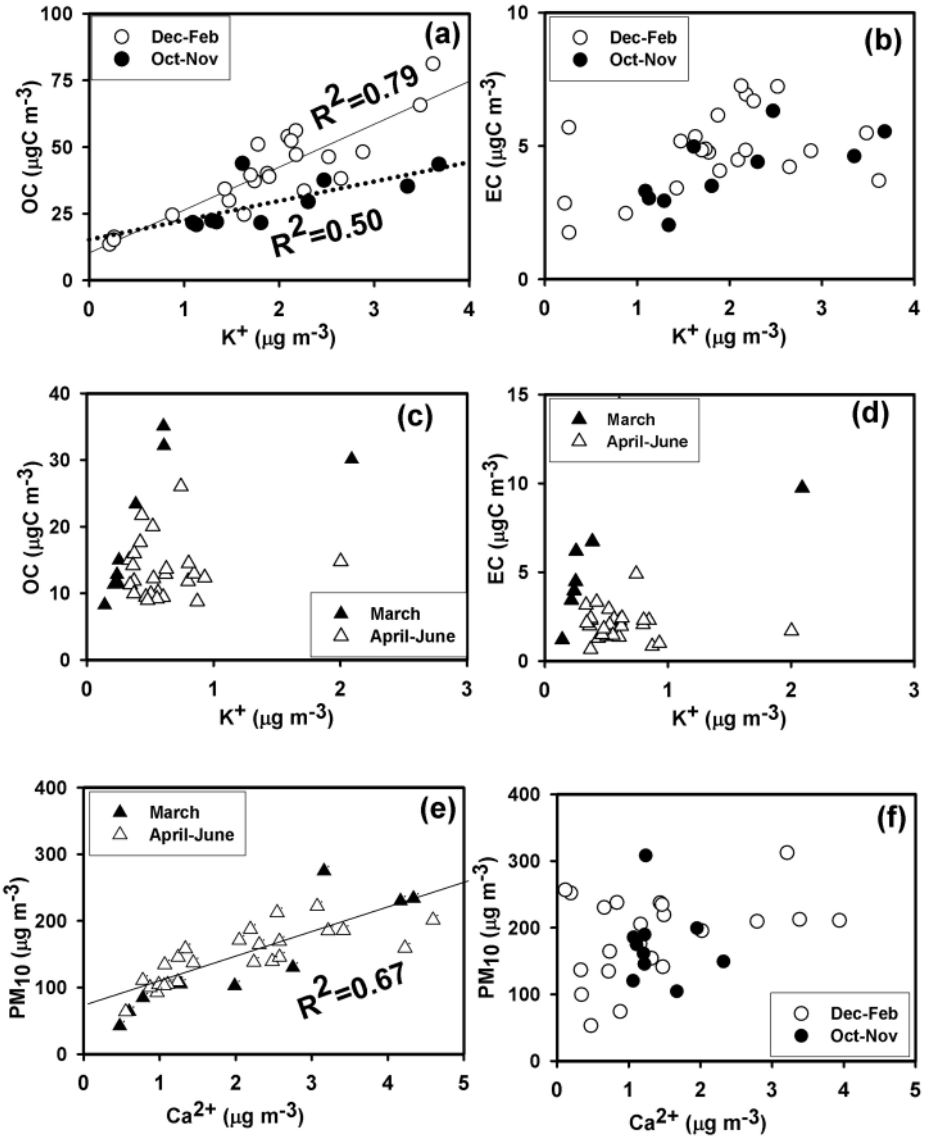

Figure 3. Scatterplots between (a) OC and K^+, (b) EC and K^+ for October–November and December–February, (c) OC and K^+, (d) EC and K^+ for March and April–June, (e) PM_{10} and Ca^{2+} for March and April–June, and (f) PM_{10} and Ca^{2+} for December–February and October–November. Relatively high concentrations of K^+ and significant correlations between OC and K^+ for the samples collected during December–February and October–November suggest biomass burning emission as a major source for OC, whereas correlation between PM_{10} and Ca^{2+} March and April–June indicates the dominance of mineral dust.

an increase in biomass burning emissions. However, the increase in mass concentrations of carbonaceous species (EC and OC) cannot be fully explained in terms of increase in their source strength. The role of meteorological conditions (wind patterns and boundary layer dynamics) is necessary to explain these variabilities. The wind speed is generally low (<2–3 ms^{-1}) and air masses are localized during winter (Figure 2). *Nair et al.* [2007] reported that the boundary layer height at the urban site (Kanpur) varied between 500 and 800 m during the observations made in December 2004. An increase in the source strength of carbonaceous aerosols and a lower boundary layer height during the winter are the main causes for the high mass concentrations of EC and OC. The WSIS also exhibit a similar seasonal variability (Figure 4c). The seasonal average WSIS concentrations account for ~24%, 9%, and 19% of PM_{10} mass during winter, summer, and post-monsoon, respectively.

[21] The OC/EC ratios exhibit a large temporal variability from sample to sample (range: 2.4–22.0; average: 7.4 ± 3.5 for n = 66). The OC/EC ratios measured in this study cover the range documented for the vehicular exhaust and biomass burning emissions [*Saarikoski et al.*, 2008]. Recent studies have suggested relatively high ratios for biomass burning emission and lower ratios for vehicular (traffic) emission [*Andreae and Merlet*, 2001; *Sandradewi et al.*, 2008].

Table 4. Monthly Average Concentrations of OC, EC, TCA, WSOC, and WSIS ($\pm 1\sigma$), Together With OC/EC and WSOC/OC Ratios at Kanpur[a]

Month	n[b]	PM_{10}	OC	EC	TCA	WSOC	WSIS	OC/EC	WSOC/OC
Jan 2007	3	215 ± 34 (213)	43.7 ± 12.4 (42.4)	5.5 ± 1.3 (5.4)	75.4 ± 19.8 (73.5)	15.0 ± 7.9 (13.6)	60.3 ± 14.4 (59.1)	8.2 ± 3.4 (7.8)	0.33 ± 0.09 (0.32)
Feb 2007	6	121 ± 55 (110)	24.0 ± 11.1 (22.0)	3.7 ± 1.8 (3.4)	42.1 ± 18.6 (38.9)	10.0 ± 5.1 (8.8)	29.4 ± 20.1 (22.5)	7.2 ± 3.1 (6.5)	0.41 ± 0.9 (0.39)
Mar 2007	8	130 ± 82 (109)	18.7 ± 10.3 (16.5)	5.3 ± 4.1 (4.2)	35.2 ± 19.2 (31.1)	6.2 ± 2.3 (5.9)	16.3 ± 9.7 (13.9)	4.8 ± 4.0 (3.9)	0.36 ± 0.09 (0.34)
Apr 2007	10	134 ± 30 (131)	16.4 ± 5.0 (15.8)	2.7 ± 1.0 (2.5)	29.0 ± 8.5 (27.9)	6.7 ± 2.3 (6.4)	17.5 ± 4.0 (17.2)	6.8 ± 2.3 (6.3)	0.43 ± 0.13 (0.41)
May 2007	10	150 ± 41 (145)	11.5 ± 2.2 (11.4)	1.7 ± 0.5 (1.6)	20.1 ± 3.8 (19.8)	6.2 ± 1.5 (6.0)	15.6 ± 4.8 (15.0)	7.5 ± 2.3 (7.2)	0.56 ± 0.10 (0.55)
Jun 2007	5	160 ± 59 (148)	11.0 ± 2.1 (10.8)	1.7 ± 0.7 (1.5)	19.2 ± 3.9 (18.9)	5.5 ± 2.3 (5.2)	21.5 ± 8.7 (20.0)	7.7 ± 4.1 (7.0)	0.50 ± 0.12 (0.49)
Oct 2007	7	160 ± 37 (156)	27.9 ± 8.8 (26.8)	3.9 ± 1.0 (3.8)	48.5 ± 14.9 (46.7)	15.5 ± 5.5 (14.7)	31.5 ± 10.3 (30.3)	7.1 ± 0.6 (7.0)	0.56 ± 0.07 (0.56)
Nov 2007	3	206 ± 88 (195)	34.5 ± 11.3 (33.1)	4.4 ± 2.2 (4.0)	59.6 ± 19.9 (57.0)	15.2 ± 2.0 (15.1)	34.4 ± 7.7 (33.9)	8.5 ± 2.4 (8.3)	0.47 ± 0.14 (0.46)
Dec 2007	5	255 ± 35 (253)	55.5 ± 15.9 (53.5)	4.4 ± 0.5 (4.4)	92.6 ± 25.2 (90.1)	21.7 ± 8.2 (20.6)	64.8 ± 13.8 (63.6)	12.8 ± 5.2 (12.1)	0.39 ± 0.07 (0.39)
Jan 2008	4	216 ± 15 (216)	46.0 ± 14.2 (44.5)	5.9 ± 1.3 (5.8)	79.4 ± 22.7 (77.2)	18.2 ± 7.3 (17.0)	49.3 ± 7.3 (48.9)	8.1 ± 3.1 (7.7)	0.40 ± 0.12 (0.39)
Feb 2008	4	160 ± 41 (158)	38.5 ± 13.4 (37.2)	5.6 ± 1.3 (5.5)	67.1 ± 18.9 (65.1)	12.3 ± 4.2 (11.6)	40.1 ± 6.3 (39.7)	6.9 ± 2.6 (6.7)	0.32 ± 0.05 (0.32)
Mar 2008	1	230	30.1	9.7	58.0	25	46.0	3.1	0.32
Annual	66	164 ± 66 (160)	25.8 ± 16.1 (21.7)	3.8 ± 2.3 (3.4)	45.0 ± 27.1 (36.8)	10.8 ± 6.6 (8.5)	30.0 ± 18.4 (24.7)	7.4 ± 3.5 (6.7)	0.44 ± 0.12 (0.46)

[a]Numbers within parentheses are median values. PM_{10}, OC, EC, TCA, WSOC, and WSIS are given in $\mu g\ m^{-3}$.
[b]Number of samples collected.

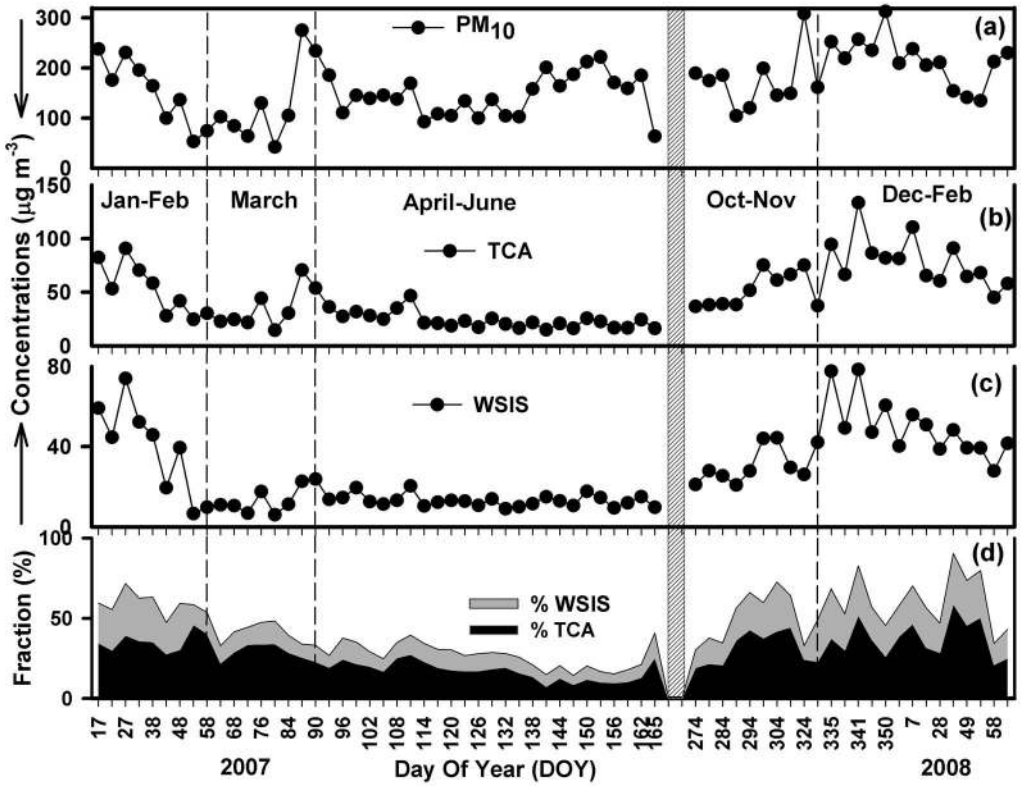

Figure 4. Temporal variability of mass concentrations of (a) PM_{10}, (b) TCA, (c) WSIS, and (d) fractional contribution of TCA and WSIS to PM_{10} during the sampling period. The time period between June and September, shown by a vertical bar, represents the monsoon period and no samples were collected.

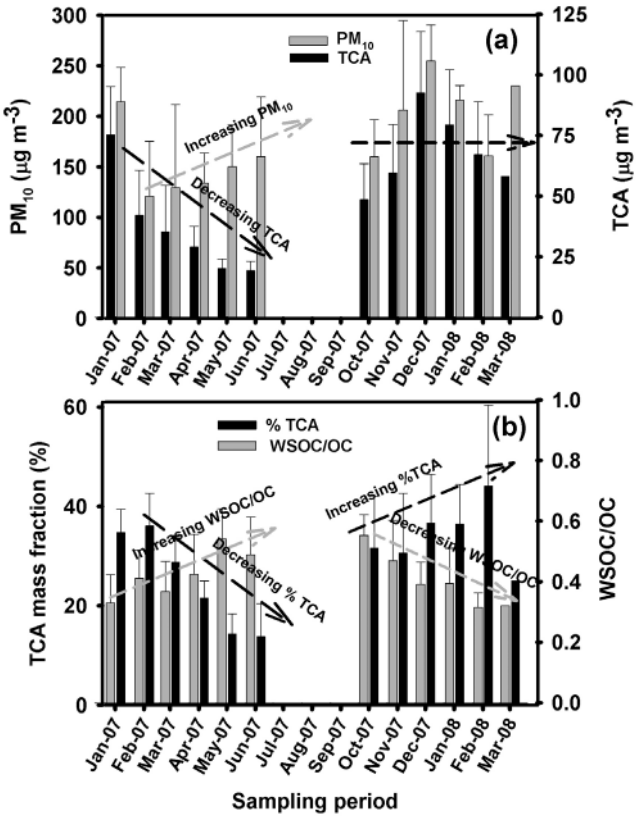

Figure 5. Monthly averaged concentrations of (a) PM_{10} and TCA and (b) TCA mass fraction and WSOC/OC ratio at an urban sampling site (Kanpur). No samples were collected during the period of southwest monsoon (July–September).

Saarikoski et al. [2008] reported an OC/EC ratio of 6.6 for biomass burning and 0.71 for vehicular emissions, whereas *Sandradewi et al.* [2008] obtained the values of 7.3 and 1.1 for these two sources, respectively. It is noteworthy that the average OC/EC ratio of 2.9 ± 0.5 in March (range: 2.4 to 3.5; $n = 7$, excluding the two high values of 6.9 and 14.1) is significantly lower than those in the winter and postmonsoon. A study by *Hopkins et al.* [2007] suggests that changes in the biomass type can result in dissimilar OC/EC ratios. A temporal shift in the emission characteristics and/or changes in the type of biomass burning (wood fuel and agricultural waste) may explain the lower OC/EC ratios in March. This has implications in the assessment of climate-relevant optical properties (such as absorption/scattering coefficient and single scattering albedo (SSA)) and direct aerosol radiative forcing on a regional scale.

3.5. Mass Concentration of WSOC and WSOC/OC Ratio

[22] The WSOC concentrations varied from 3.3 to 33.5 μgC m^{-3} and the WSOC/OC ratios ranged from 0.21 to 0.70 during the entire sampling period (Figure 6c). The regression plot between WSOC and OC shows a significant linear relationship for the samples collected during the winter (Figure 7a). However, a large scatter in the data for the samples collected during summer months (Figure 7b) indicates contribution of WSOC and OC from multiple sources and/or secondary organic aerosols. The monthly averaged EC, OC, and WSOC mass concentrations along with the WSOC/OC ratios are given in Table 4. The average WSOC/OC ratios are higher in the samples collected during summer and postmonsoon. The median (average $\pm 1\sigma$) values of WSOC/OC ratios in the winter, summer, and postmonsoon are 0.37 (0.37 ± 0.09), 0.48 (0.51 ± 0.13), and 0.53 (0.54 ± 0.09), respectively. The WSOC/OC ratios (this study) during winter are similar to those reported (0.32 ± 0.14) from an urban site (Hisar) in the IGP during a field campaign in December 2004 [*Rengarajan et al.*, 2007]. *Miyazaki et al.* [2007] reported that WSOC and OC concentrations measured at Gosan, Korea, show similar temporal trend, with WSOC/OC ratios ranging from 0.02 to 0.66 (average: 0.30 ± 0.14) for different air masses. Likewise, relatively high WSOC/OC ratios (0.34 ± 0.13) have been reported for the air masses over mainland China. Furthermore, *Ho et al.* [2006] reported that WSOC account for ~50–70% of OC at Hok Tsui (regional), whereas its contribution is only about one third of OC at a road site (Polytechnic University) and Kuang Tong (urban residential site).

[23] In general, relatively high WSOC/OC ratios during summer indicate contribution from SOA due to an increase in the photochemical activity and/or aging of the aerosols during transport [*Pio et al.*, 2007]. The mass concentration of WSOC is largely attributed to the atmospheric oxidation of volatile organic compounds via reactions with strong oxidants (ozone and peroxide radicals) through the gas phase conversion and the formation of SOA [*Miyazaki et al.*, 2007; *Pio et al.*, 2007; *Weber et al.*, 2007]. In addition, a significant fraction of WSOC is derived from particulate OC, which is produced from biomass burning and/or vehicular emissions. For example, *Saarikoski et al.* [2008] reported a WSOC/OC ratio of 0.40 for the biomass burning and a lower value of 0.27 for emissions from vehicular traffic. *Pio et al.* [2007] suggested relatively lower WSOC/OC ratios for the urban locations (near to the source region of the emissions) and an increase in the ratio during the transport at remote sites due to aging of the aerosols. During winter, the aerosol samples are more influenced by the nearby source regions and the contribution of SOA is minor hence the lower WSOC/OC ratios. The higher ratios during summer and postmonsoon provide evidence for the enhanced SOA formation in the IGP.

3.6. Intercomparison of Mass Concentrations of EC and OC

[24] An extensive land campaign was carried out during winter (December 2004) over the Indo-Gangetic Plain wherein measurements of BC mass concentration (along with several other chemical and optical properties) were carried out [*Nair et al.*, 2007; *Ramachandran et al.*, 2006; *Rengarajan et al.*, 2007; *Tare et al.*, 2006; *Tripathi et al.*, 2005]. These studies reported a large-scale heterogeneity and spatiotemporal variability in aerosol chemical and optical properties over the IGP. The OC and EC mass concentrations at Kanpur during winter and postmonsoon seasons are similar to those at Hisar (Table 5). However, OC and EC concentrations are two to three times lower in the summer months. A comparison of measured OC and EC concentrations at Kanpur during 2007–2008 (this study) and

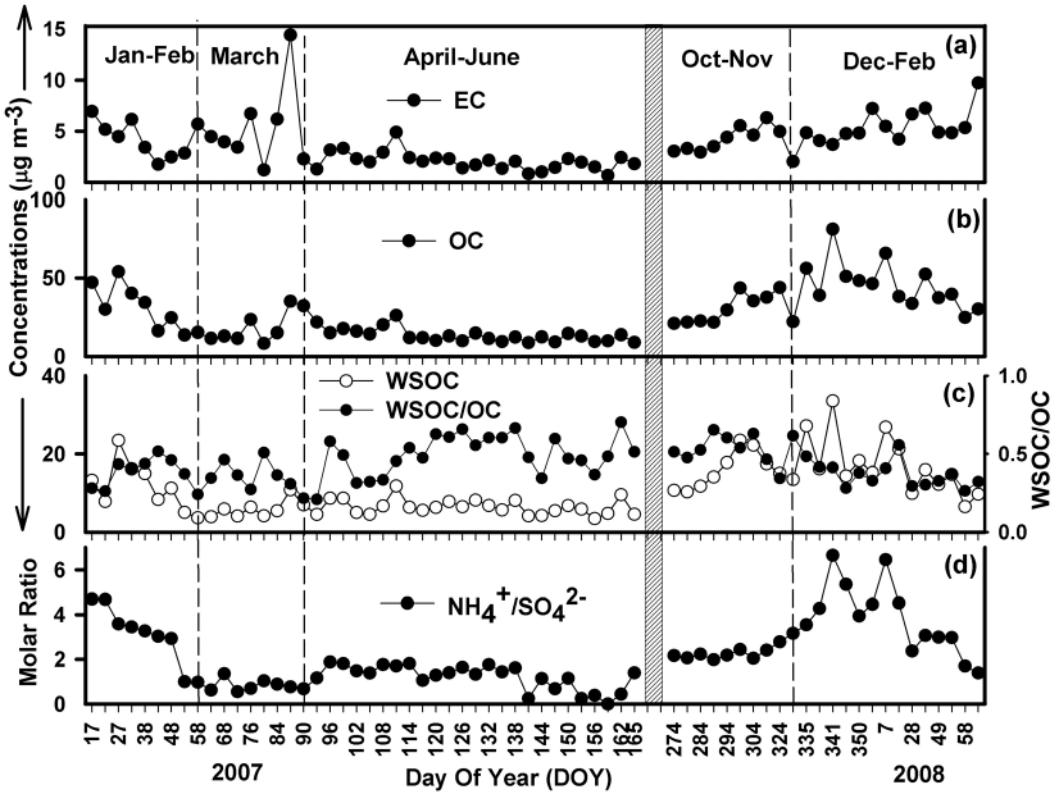

Figure 6. Temporal variability of the concentrations of carbonaceous species: (a) EC, (b) OC, (c) WSOC and WSOC/OC ratio, and (d) NH_4^+/SO_4^{2-} molar ratio at Kanpur. The time period between June and September, shown by a vertical bar, represents the monsoon period and no samples were collected.

those reported in the literature from different sampling locations in India are given in Table 5. Filter-based measurements of OC and EC are limited over Indian regions [*Rengarajan et al.*, 2007; *Venkataraman et al.*, 2002]; however, BC measurements using an Aethalometer have been extensively made to document the spatiotemporal variability. Over urban locations, BC concentrations are generally less than 15 μgC m^{-3} (Table 5), however, it can be as high as 60 μgC m^{-3} at some locations [*Ganguly et al.*, 2006; *Latha and Badarinath*, 2003]. *Tripathi et al.* [2005] reported that BC mass concentration at Kanpur varied from 6 to 20 μgC m^{-3} during the field campaign (December 2004) and resulted in a low value of 0.76 for SSA. During the same field campaign, *Ganguly et al.* [2006] reported that BC mass concentration was as high as 60 μgC m^{-3} at Delhi (an urban location) with an average value of 29 ± 14 μgC m^{-3}, resulting in a further lower value of 0.68 for SSA.

[25] Although EC constitutes only a minor fraction of PM_{10} mass, it is one of the major absorbing particulate species of solar radiation. Thus, the EC/PM_{10} mass ratio can provide a qualitative assessment of the absorbing nature of aerosols and helps to understand the radiative impact of EC. In general, the EC/PM_{10} ratio varies from 3 to 10% over the urban locations in India [*Babu and Moorthy*, 2002; *Babu et al.*, 2002], but it can be as high as 15% during winter in some parts of the IGP [*Ganguly et al.*, 2006; *Tripathi et al.*, 2005]. The EC/PM_{10} mass ratio at Kanpur exhibit a large temporal variability (range: 0.4 to 7.7% of PM_{10}; average: 2.5 ± 1.5% of PM_{10}) during the study period. The EC/PM_{10} mass ratios are slightly higher during winter (range: 1.4% to 7.7%; average: 2.9 ± 1.5% of PM_{10}) and postmonsoon season (range: 1.4% to 7.7%; average: 2.5 ± 1.1% of PM_{10}) and lower during summer (range: 0.4% to 2.9%; average: 1.6 ± 0.8% of PM_{10}). However, the highest EC/PM_{10} ratio is obtained for the samples collected during spring season (range: 1.0% to 5.9%; average: 4.3 ± 1.5% of the PM_{10}). In addition to meteorological conditions, such large variability in the EC/PM_{10} ratio at Kanpur can be attributed to the changes in the source strength of carbonaceous and mineral aerosols. Earlier studies reported in the literature have suggested relatively low EC/PM_{10} ratios over semi-arid and high-altitude locations compared to those over urban environments [*Hegde et al.*, 2007; *Pant et al.*, 2006; *Ram et al.*, 2008]. The seasonal variability in the mass concentrations of absorbing EC and EC/PM_{10} ratios observed in this study can have significant influence on the estimation of SSA and direct aerosol radiative forcing on a regional scale.

3.7. Inorganic Constituents and Neutralization of Acidic Species (SO_4^{2-} and NO_3^-)

[26] The seasonal average ($\pm 1\sigma$) concentrations of the measured ionic species are summarized in Table 3; SO_4^{2-}, NO_3^-, and HCO_3^- are the major contributors to WSIS, followed by contribution from NH_4^+, K^+, and Ca^{2+}. The contribution of WSIS to PM_{10} mass varies from 6% to 32% during the 1 year sampling period (Figure 4d) and the annual average WSIS concentration accounts for ~15% of the PM_{10} mass. The mass concentrations of SO_4^{2-}, NO_3^-, K^+, and NH_4^+ are significantly higher during winter and postmonsoon, while the mass concentrations of Ca^{2+}, Mg^{2+}, and

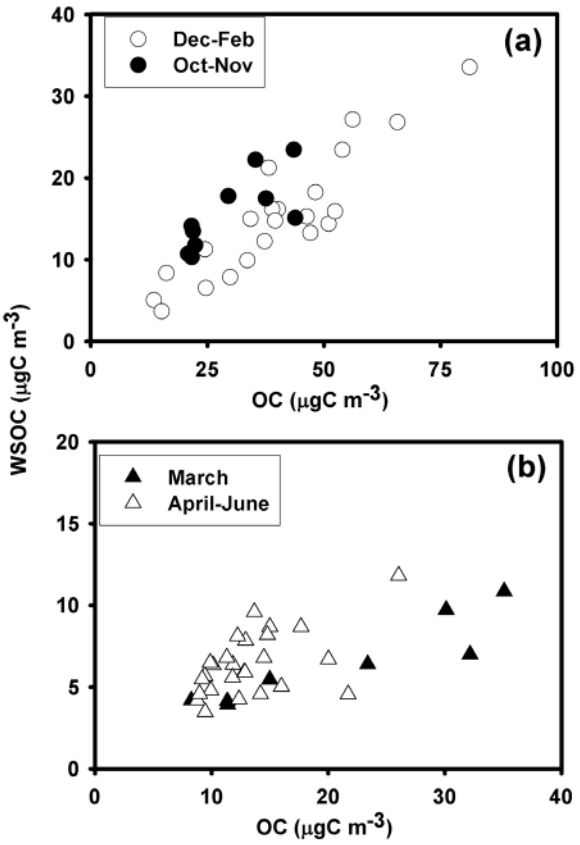

Figure 7. Scatterplots between WSOC and OC for (a) December–February and October–November and (b) March and April–June.

HCO_3^- are higher in the summer season (Table 3). The seasonal variability in the ionic species concentrations is also reflected in the abundant WSIS concentration during winter and postmonsoon (Figure 4c).

[27] The ratio of Σ^+ (sum of cations, μeq m^{-3}) to Σ^- (sum of anions, μeq m^{-3}) at the sampling site varies from 0.68 to 1.25 (average: 1.01 ± 0.12, n = 65, excluding one data point with a ratio of 0.31). Furthermore, the linear regression plot between Σ^+ and Σ^- shows a good correlation with a slope close to unity and near-zero intercept ($\Sigma^+ = 0.97 \times \Sigma^- + 0.02$, $R^2 = 0.97$, $n = 65$). The acidic species (SO_4^{2-} and NO_3^-) produced by the oxidation of the gaseous precursors (SO_2 and NO_x) in the atmosphere are neutralized by the ammonia and mineral aerosols [*Han et al.*, 2007]. In ammonia (NH_3)-rich environments, neutralization of the sulfuric acid (H_2SO_4) is favored, forming ammonium sulfate [$(NH_4)_2SO_4$] and/or ammonium hydrosulfate [NH_4HSO_4] [*Pathak et al.*, 2009]. The NH_4^+/SO_4^{2-} molar ratios for the formation of $(NH_4)_2SO_4$ and NH_4HSO_4 are 2:1 and 1:1, respectively. The NH_4^+/SO_4^{2-} molar ratio in this study shows a large variability (range: 0.24 to 6.6; Figure 6d); with lower ratios typical of the samples collected during March and the summer months. The low NH_4^+/SO_4^{2-} molar ratio emphasizes the role of Ca^{2+} and Mg^{2+} in the neutralization process of acidic species during the summer. In order to get a better insight of the neutralization process, we have calculated the neutralization factors (NF) for NH_4^+, Ca^{2+}, and Mg^{2+}. The NF of a cation "X" is defined by the following equation,

$$NF(X) = \frac{[X]}{\left[NO_3^-\right] + \left[nss - SO_4^{2-}\right]}, \quad (1)$$

where the concentration of each ionic species in equation (1) is expressed in terms of the equivalent unit (i.e., μeq m^{-3}).

Table 5. Comparison of OC and EC (or BC) Concentrations and OC/EC Ratios Over Indian Regions

Sampling Time	Location	Type	Longitude °N	Latitude °E	Elevation (m amsl[a])	OC (μg m^{-3})	EC or BC (μg m^{-3})	OC/EC	References
Jan–Feb 2007 and Dec 2007 to Feb 2008	Kanpur	Urban	26.5	80.3	142	40.4 ± 16.6	4.9 ± 1.5	8.7 ± 3.9	This study
Mar 2007						19.9 ± 10.3	5.8 ± 4.1	4.6 ± 3.8	This study
Apr–Jun 2007						13.4 ± 4.3	2.1 ± 0.9	7.3 ± 3.2	This study
Oct–Nov 2007						29.8 ± 9.5	4.1 ± 1.3	7.5 ± 1.4	This study
Dec 2004	Hisar	Urban	29.2	75.7	219	33 ± 17.9	3.8 ± 1.4	8.5 ± 2.2	*Rengarajan et al.* [2007]
Feb 2005 to Jun 2007	Manora Peak	High altitude	29.4	79.5	1950	8.7 ± 4.5	1.1 ± 0.7	8.4 ± 2.8	*Ram et al.* [2008]
Jun 2005 to Feb 2006	Mt Abu	High altitude	24.6	72.7	1700	3.7 ± 2.4	0.5 ± 0.5	6.1 ± 2.0	*Ram et al.* [2008]
Jan–Mar 1999	Mumbai[b]	Urban	18.9	72.9	0	37.3 ± 10.5	12.4 ± 5.1	3.1 ± 0.5	*Venkataraman et al.* [2002]
Jan–Mar 2000	Mumbai[b]	Urban	18.9	72.9	0	25.3 ± 9.9	12.6 ± 3.0	2.0 ± 0.3	*Venkataraman et al.* [2002]
Dec 2004	Manora Peak[b]	High altitude	29.4	79.5	1950		1.4 ± 1.0		*Pant et al.* [2006]
Dec 2004	Kanpur[b]	Urban	26.5	80.3	142		6.0–20.0		*Tripathi et al.* [2005]
Aug 2000 to Oct 2001	Trivandrum[b]	Urban	8.57	77.0	1		4.0–8.0		*Babu and Moorthy* [2002]
Jan–Jul 2003	Hyderabad[b]	Urban	17.2	78.3	500		0.5–68		*Latha and Badarinath* [2003]
Oct–Dec 2001	Bangalore[b]	Urban	13.0	77.6	960		0.4–10.2		*Babu et al.* [2002]
Dec 2004	Delhi[b]	Urban	28.6	77.2	239		29.0 ± 14.0		*Ganguly et al.* [2006]
Dec 2004	Kharaghpur[b]	Urban	22.3	87.3	30		8.0–28.0		*Nair et al.* [2007]

[a]amsl, above mean sea level.
[b]Aethalometer BC data.

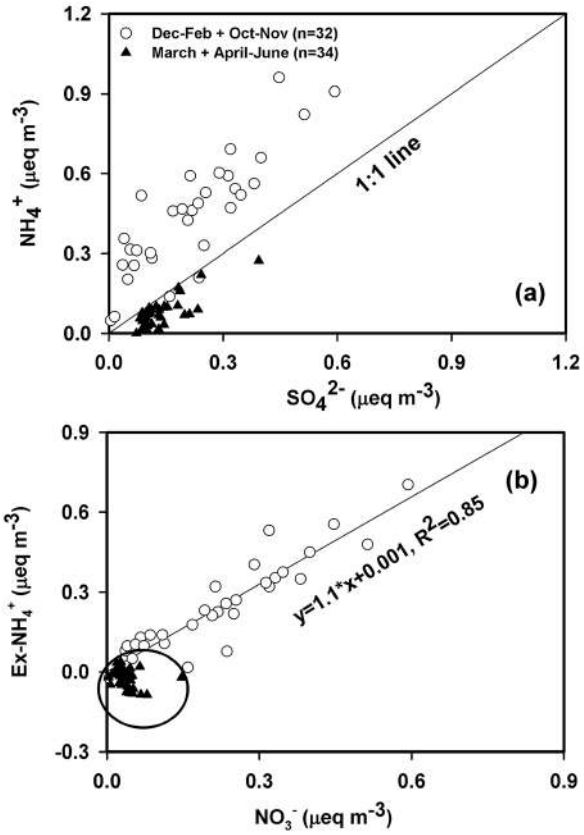

Figure 8. Scatterplots between (a) NH_4^+ and SO_4^{2-}, indicating presence of excess NH_4^+ in the samples collected during December–February and October–November. (b) Excess NH_4^+ and particulate NO_3^-, indicating the existence of ammonium nitrate (NH_4NO_3) during December–February and October–November. Negative values (circled data points and excluded from regression analysis) on *y* axis indicates deficiency of NH_4^+ in spring and summer samples. "n" represents the number of aerosol samples collected in each time period.

Non-sea salt sulfate, nss-SO_4^{2-}, defined as Total [SO_4^{2}] − 0.2514 × [Na^+], represents the concentration that is corrected for the contribution from sea salts [*Chester*, 1990]. The calculated NF for NH_4^+, Ca^{2+}, and Mg^{2+} are presented in Table 3. It can be inferred that NH_4^+ is the major neutralizing agent for the acidic species in the winter and postmonsoon (average NF values are 0.87 and 0.88, respectively), whereas Ca^{2+} is the major neutralizing agent in the summer (average NF = 0.53).

[28] The formation of ammonium nitrate (NH_4NO_3) is favored at a lower ambient temperature (due to the volatile nature of NH_4NO_3) in the presence of high ammonia and HNO_3 concentrations rather than the neutralization of acidic sulfate by the ammonia. Recently, *Pathak et al.* [2009] suggested that the formation of NH_4NO_3, via gas phase reaction of NH_3 and HNO_3, is important for the molar ratio of NH_4^+/SO_4^{2-} greater than 1.5. The scatterplot between NH_4^+ and SO_4^{2-} is presented in Figure 8a, indicating the presence of excess NH_4^+ and its existence as NH_4NO_3 salt. The $[NH_4^+]_{Excess}$ (where $[NH_4^+]_{Excess}$ = {$[NH_4^+/SO_4^{2-}]_{molar}$ − 1.5} × [SO_4^{2-}]) calculated for the samples collected during winter and postmonsoon is positive (except for the two samples collected in late February 2007; Figure 8a). Furthermore, $[NH_4^+]_{Excess}$ and NO_3^- also exhibit a linear positive relationship for these samples (R^2 = 0.85; Figure 8b), suggesting an ammonia-rich environment. The major sources of NH_3 in the IGP are human and animal excretion during the metabolism processes and those emitted from the fertilizers used for agriculture purposes. The agriculture activity is widespread in the Gangetic Plain and the use of fertilizers is very common. Among the commonly used fertilizers, urea (NH_2CONH_2) comprises nearly 45% of the nitrogen (wt/wt), and the decomposition of urea produces ammonia, which is mainly trapped in the lower atmosphere due to the shallow boundary layer height, leading to an ammonia-rich environment during winter. Large scatter and relatively low concentrations of NH_4^+, representing ammonia deficiency, are seen in the majority of the samples (>80%) collected during the summer.

4. Conclusions and Implications

[29] A 1 year study on the chemical characteristics of ambient aerosols (PM_{10}) from an urban location (Kanpur) in the Indo-Gangetic Plain has led us to make the following conclusions:

[30] 1. The temporal variability in the atmospheric concentrations of carbonaceous species (EC and OC) is significantly pronounced over the Gangetic Plain due to a shallow boundary layer height and the dominance of biomass burning (wood fuel and agricultural waste) emissions during the winter. In contrast, the long-range transport of mineral dust and its contribution to the aerosol composition is conspicuous in the summer. Therefore, a decrease in the concentration of EC and EC/PM_{10} mass ratio has implications in the assessment of aerosol radiative forcing on a temporal and regional scale.

[31] 2. On an annual basis, about 45% of OC is water soluble and an increase in the WSOC/OC ratios (during summer) provides evidence for the formation of secondary organic aerosols. The representative OC/EC and WSOC/OC ratios for the central part of the Gangetic Plain are 8.7 ± 3.9 and 0.37 ± 0.09 in winter and 7.3 ± 3.2 and 0.50 ± 0.10 in summer.

[32] 3. The efficient neutralization of H_2SO_4 by NH_3 in the winter and a NH_4^+/SO_4^{2-} molar ratio greater than 2 suggest the formation of $(NH_4)_2SO_4$ and NH_4HSO_4 salts, whereas their molar ratio is less than 1 during summer. These results have implications to the formation of secondary particulate species over urban regions, which degrade the air quality and visibility.

[33] To sum up, results obtained from our study have important implications to the atmospheric processing (aging!) of carbonaceous aerosols. In the high-acid environment of the Gangetic Plain, as evident based on the high concentration of sulfate aerosols during winter, elemental carbon may undergo marked changes in the morphological features and mass growth and, thus, may cause significant enhancement in the scattering properties.

[34] **Acknowledgments.** We thank Sanjay Baxala for the help in the collection of aerosol samples. The funding support received from Indian Space Research Organization-Geosphere Biosphere Programme (Bangaluru, India) is thankfully acknowledged. S.N.T. also acknowledges financial support from Department of Science and Technology ICRP Programme. The

authors gratefully acknowledge the NOAA ARL for the provision of the HYSPLIT transport and dispersion model and/or READY website (http://www.arl.noaa.gov/ready.php) used in this paper.

References

Andreae, M. O. (1983), Soot carbon and excess fine potassium: Long-range transport of combustion-derived aerosols, *Science*, *220*(4602), 1148–1151.

Andreae, M. O., and P. Merlet (2001), Emission of trace gases and aerosols from biomass burning, *Global Biogeochem. Cycles*, *15*(4), 955–966.

Babu, S. S., and K. K. Moorthy (2002), Aerosol black carbon over a tropical coastal station in India, *Geophys. Res. Lett.*, *29*(23), 2098, doi:10.1029/2002GL015662.

Babu, S. S., S. K. Satheesh, and K. K. Moorthy (2002), Aerosol radiative forcing due to enhanced black carbon at an urban site in India, *Geophys. Res. Lett.*, *29*(18), 1880, doi:10.1029/2002GL015826.

Bond, T. C., E. Bhardwaj, R. Dong, R. Jogani, S. Jung, C. Roden, D. G. Streets, and N. M. Trautmann (2007), Historical emissions of black and organic carbon aerosol from energy-related combustion, 1850–2000, *Global Biogeochem. Cycles*, *21*, GB2018, doi:10.1029/2006GB002840.

Cao, J. J., S. C. Lee, K. F. Ho, X. Y. Zhang, S. C. Zou, K. Fung, J. C. Chow, and J. G. Watson (2003), Characteristics of carbonaceous aerosol in Pearl River Delta Region, China, during 2001 winter period, *Atmos. Environ.*, *37*(11), 1451–1460.

Chester, R. (1990), *Marine Geochemistry*, 698 pp., Unwin Hyman, London.

Chinnam, N., S. Dey, S. N. Tripathi, and M. Sharma (2006), Dust events in Kanpur, northern India: Chemical evidence for source and implications to radiative forcing, *Geophys. Res. Lett.*, *33*, L08803, doi:10.1029/2005GL025278.

Chowdhury, Z., M. Zheng, J. J. Schauer, R. J. Sheesley, L. G. Salmon, G. R. Cass, and A. G. Russell (2007), Speciation of ambient fine organic carbon particles and source apportionment of PM2.5 in Indian cities, *J. Geophys. Res.*, *112*, D15303, doi:10.1029/2007JD008386.

Dey, S., and S. N. Tripathi (2008), Aerosol direct radiative effects over Kanpur in the Indo-Gangetic basin, northern India: Long-term (2001–2005) observations and implications to regional climate, *J. Geophys. Res.*, *113*, D04212, doi:10.1029/2007JD009029.

Fuzzi, S., et al. (2006), Critical assessment of the current state of scientific knowledge, terminology, and research needs concerning the role of organic aerosols in the atmosphere, climate, and global change, *Atmos. Chem. Phys.*, *6*, 2017–2038.

Ganguly, D., A. Jayaraman, T. A. Rajesh, and H. Gadhavi (2006), Wintertime aerosol properties during foggy and non-foggy days over urban center Delhi and their implications for shortwave radiative forcing, *J. Geophys. Res.*, *111*, D15217, doi:10.1029/2005JD007029.

Ganguly, D., P. Ginoux, V. Ramaswamy, D. M. Winker, B. N. Holben, and S. N. Tripathi (2009), Retrieving the composition and concentration of aerosols over the Indo-Gangetic basin using CALIOP and AERONET data, *Geophys. Res. Lett.*, *36*, L13806, doi:10.1029/2009GL038315.

Han, L., G. Zhuang, S. Cheng, and J. Li (2007), The mineral aerosol and its impact on urban pollution aerosols over Beijing, China, *Atmos. Environ.*, *41*, 7533–7546.

Hegde, P., P. Pant, M. Naja, U. C. Dumka, and R. Sagar (2007), South Asian dust episode in June 2006: Aerosol observations in the central Himalayas, *Geophys. Res. Lett.*, *34*, L23802, doi:10.1029/2007GL030692.

Ho, K. F., S. C. Lee, J. J. Cao, Y. S. Li, J. C. Chow, J. G. Watson, and K. Fung (2006), Variability of organic and elemental carbon, water soluble organic carbon, and isotopes in Hong Kong, *Atmos. Chem. Phys.*, *6*, 4569–4576.

Hopkins, R. J., K. Lewis, Y. Desyaterik, Z. Wang, A. V. Tivanski, W. P. Arnott, A. Laskin, and M. K. Gilles (2007), Correlations between optical, chemical, and physical properties of biomass burn aerosols, *Geophys. Res. Lett.*, *34*, L18806, doi:10.1029/2007GL030502.

Jethva, H., S. K. Satheesh, and J. Srinivasan (2005), Seasonal variability of aerosols over the Indo-Gangetic basin, *J. Geophys. Res.*, *110*, D21204, doi:10.1029/2005JD005938.

Latha, K. M., and K. V. S. Badarinath (2003), Black carbon aerosols over tropical urban environment: A case study, *Atmos. Res.*, *69*, 125–133.

Lin, C.-Y., Z. Wang, W.-N. Chen, S.-Y. Chang, C. C. K. Chou, N. Sugimoto, and X. Zhao (2007), Long-range transport of Asian dust and air pollutants to Taiwan: Observed evidence and model simulation, *Atmos. Chem. Phys.*, *7*(2), 423–434.

Mishra, S. K., and S. N. Tripathi (2008), Modeling optical properties of mineral dust over the Indian Desert, *J. Geophys. Res.*, *113*, D23201, doi:10.1029/2008JD010048.

Miyazaki, Y., Y. Kondo, S. Han, M. Koike, D. Kodama, Y. Komazaki, H. Tanimoto, and H. Matsueda (2007), Chemical characteristics of water-soluble organic carbon in the Asian outflow, *J. Geophys. Res.*, *112*, D22S30, doi:10.1029/2007JD009116.

Miyazaki, Y., S. G. Aggarwal, K. Singh, P. K. Gupta, and K. Kawamura (2009), Dicarboxylic acids and water-soluble organic carbon in aerosols in New Delhi, India in winter: Characteristics and formation processes, *J. Geophys. Res.*, *114*, D22S30, doi:10.1029/2007JD009116.

Nair, V. S., et al. (2007), Wintertime aerosol characteristics over the Indo-Gangetic Plain (IGP): Impacts of local boundary layer processes and long-range transport, *J. Geophys. Res.*, *112*, D13205, doi:10.1029/2006JD008099.

Novakov, T., S. Menon, T. W. Kirchstetter, D. Koch, and J. E. Hansen (2005), Aerosol organic carbon to black carbon ratios: Analysis of published data and implications for climate forcing, *J. Geophys. Res.*, *110*, D21205, doi:10.1029/2005JD005977.

Pant, P., P. Hegde, U. C. Dumka, R. Sagar, S. K. Satheesh, K. K. Moorthy, A. Saha, and M. K. Srivastava (2006), Aerosol characteristics at a high-altitude location in central Himalayas: Optical properties and radiative forcing, *J. Geophys. Res.*, *111*, D17206, doi:10.1029/2005JD006768.

Pathak, R. K., W. S. Wu, and T. Wang (2009), Summertime PM2.5 ionic species in four major cities of China: Nitrate formation in an ammonia-deficient atmosphere, *Atmos. Chem. Phys.*, *9*, 1711–1722.

Pio, C. A., et al. (2007), Climatology of aerosol composition (organic versus inorganic) at nonurban sites on a west-east transect across Europe, *J. Geophys. Res.*, *112*, D23S02, doi:10.1029/2006JD008038.

Ram, K., and M. M. Sarin (2010), Spatio-temporal variability in atmospheric abundances of EC, OC and WSOC over northern India, *J. Aerosol Sci.*, *41*(1), 88–98.

Ram, K., M. M. Sarin, and P. Hegde (2008), Atmospheric abundances of primary and secondary carbonaceous species at two high-altitude sites in India: Sources and temporal variability, *Atmos. Environ.*, *42*(28), 6785–6796.

Ramachandran, S., R. Rengarajan, A. Jayaraman, M. M. Sarin, and S. K. Das (2006), Aerosol radiative forcing during clear, hazy, and foggy conditions over a continental polluted location in north India, *J. Geophys. Res.*, *111*, D20214, doi:10.1029/2006JD007142.

Rastogi, N., and M. M. Sarin (2006), Chemistry of aerosols over a semi-arid region: Evidence for acid neutralization by mineral dust, *Geophys. Res. Lett.*, *33*, L23815, doi:10.1029/2006GL027708.

Rengarajan, R., M. M. Sarin, and A. K. Sudheer (2007), Carbonaceous and inorganic species in atmospheric aerosols during wintertime over urban and high-altitude sites in North India, *J. Geophys. Res.*, *112*, D21307, doi:10.1029/2006JD008150.

Saarikoski, S., H. Timonen, K. Saarnio, M. Aurela, L. Jarvi, P. Keronen, V.-M. Kerminen, and R. Hillamo (2008), Sources of organic carbon in fine particulate matter in northern European urban air, *Atmos. Chem. Phys.*, *8*, 6281–6295.

Sandradewi, J., A. S. H. Prévôt, S. Szidat, N. Perron, M. Rami Alfarra, V. A. Lanz, E. Weingartner, and U. Baltensperger (2008), Using aerosol light absorption measurements for the quantitative determination of wood burning and Traffic emission contributions to particulate matter, *Environ. Sci. Technol.*, *42*(9), 3316–3323.

Sheesley, R. J., J. J. Schauer, Z. Chowdhury, G. R. Cass, and B. R. T. Simoneit (2003), Characterization of organic aerosols emitted from the combustion of biomass indigenous to South Asia, *J. Geophys. Res.*, *108*(D9), 4285, doi:10.1029/2002JD002981.

Singh, S., S. Nath, R. Kohli, and R. Singh (2005), Aerosols over Delhi during pre-monsoon months: Characteristics and effects on surface radiation forcing, *Geophys. Res. Lett.*, *32*, L13808, doi:10.1029/2005GL023062.

Streets, D. G., T. C. Bond, T. Lee, and C. Jang (2004), On the future of carbonaceous aerosol emissions, *J. Geophys. Res.*, *109*, D24212, doi:10.1029/2004JD004902.

Tare, V., et al. (2006), Measurements of atmospheric parameters during Indian Space Research Organization Geosphere Biosphere Program Land Campaign II at a typical location in the Ganga Basin: 2. Chemical properties, *J. Geophys. Res.*, *111*, D23210, doi:10.1029/2006JD007279.

Tripathi, S. N., S. Dey, V. Tare, and S. K. Satheesh (2005), Aerosol black carbon radiative forcing at an industrial city in northern India, *Geophys. Res. Lett.*, *32*, L08802, doi:10.1029/2005GL022515.

Turpin, B. J., and H.-J. Lim (2001), Species contributions to PM2.5 mass concentrations: Revisiting common assumptions for estimating organic mass, *Aerosol Sci. Technol.*, *35*(1), 602–610.

Venkataraman, C., C. K. Reddy, S. Josson, and M. S. Reddy (2002), Aerosol size and chemical characteristics at Mumbai, India, during the INDOEX-IFP (1999), *Atmos. Environ.*, *36*(12), 1979–1991.

Weber, R. J., et al. (2007), A study of secondary organic aerosol formation in the anthropogenic-influenced southeastern United States, *J. Geophys. Res.*, *112*, D13302, doi:10.1029/2007JD008408.

K. Ram and M. M. Sarin, Geosciences Division, Navarangpura, Physical Research Laboratory, Ahmedabad, India-380 009. (sarin@prl.res.in; kirpa@prl.res.in)

S. N. Tripathi, Department of Civil Engineering, Indian Institute of Technology, Kanpur, India, 208 016. (snt@iitk.ac.in)